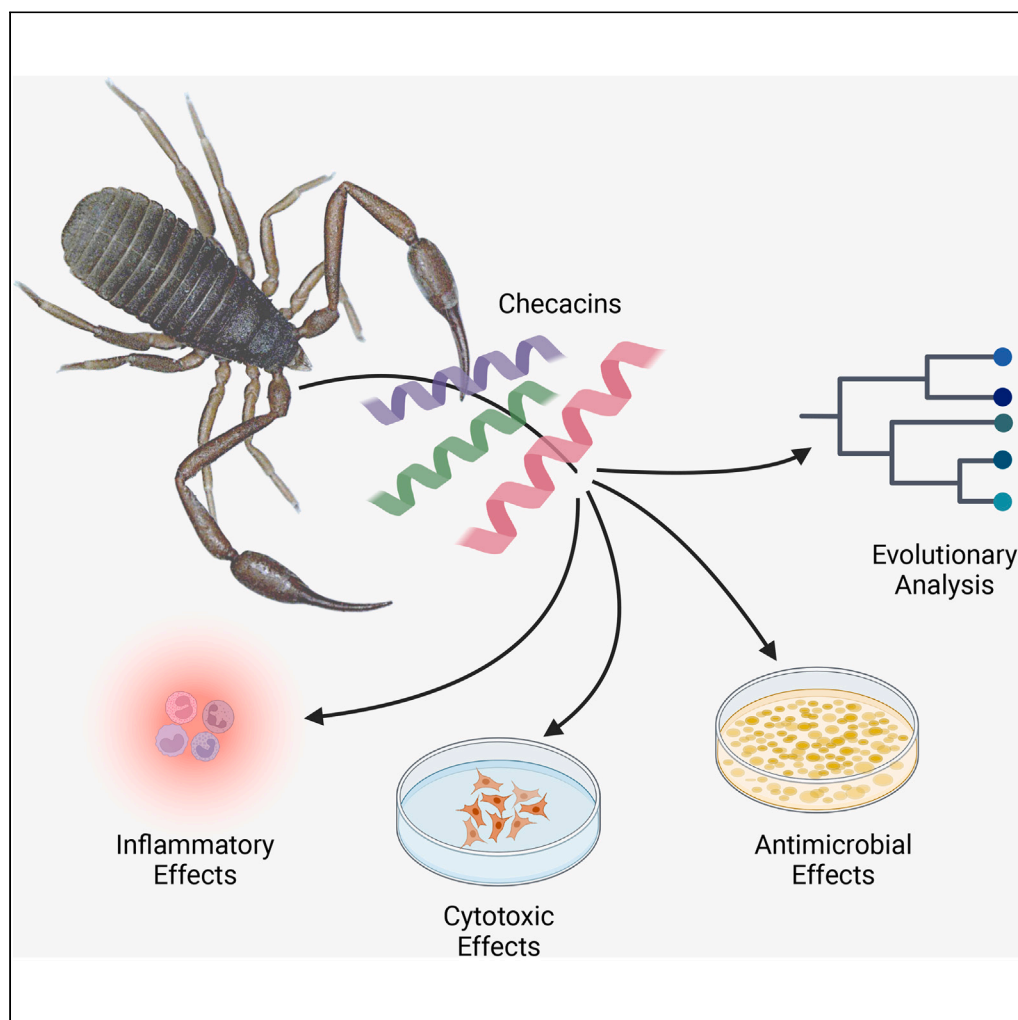


Article

Determining the pharmacological potential and biological role of linear pseudoscorpion toxins via functional profiling



Pelin Erkoç,
Susanne
Schiffmann,
Thomas Ulshöfer,
..., Andreas
Vilcinskis, Robert
Fürst, Tim
Lüddecke

r.fuerst@lmu.de (R.F.)
tim.lueddecke@ime.fraunhofer.
de (T.L.)

Highlights

Pseudoscorpions belong to the least studied venomous animals on earth

A first bioactivity profiling of Checacins, an entire pseudoscorpion toxin family

Checacins show potent activity against pathogenic bacteria including MRSA

They may have evolved to defend the venom gland against microbial colonization

Erkoç et al., iScience 27, 110209
July 19, 2024 © 2024 The
Authors. Published by Elsevier
Inc.
[https://doi.org/10.1016/
j.isci.2024.110209](https://doi.org/10.1016/j.isci.2024.110209)

Article

Determining the pharmacological potential and biological role of linear pseudoscorpion toxins via functional profiling

Pelin Erkoc,^{1,2,9} Susanne Schiffmann,^{2,3,9} Thomas Ulshöfer,^{2,3} Marina Henke,^{2,3} Michael Marnier,⁴ Jonas Krämer,^{5,6} Reinhard Predel,⁵ Till F. Schäberle,^{4,6,7} Sabine Hurka,^{2,4} Ludwig Dersch,^{2,4} Andreas Vilcinskas,^{2,4,6} Robert Fürst,^{2,8,*} and Tim Lüddecke^{2,4,10,*}

SUMMARY

Arthropod venoms contain bioactive molecules attractive for biomedical applications. However, few of these have been isolated, and only a tiny number has been characterized. Pseudoscorpions are small arachnids whose venom has been largely overlooked. Here, we present the first structural and functional assessment of the checacin toxin family, discovered in the venom of the house pseudoscorpion (*Chelifer cancroides*). We combined *in silico* and *in vitro* analyses to establish their bioactivity profile against microbes and various cell lines. This revealed inhibitory effects against bacteria and fungi. We observed cytotoxicity against specific cell types and effects involving second messengers. Our work provides insight into the biomedical potential and evolution of pseudoscorpion venoms. We propose that plesiotypic checacins evolved to defend the venom gland against infection, whereas apotypic descendants evolved additional functions. Our work highlights the importance of considering small and neglected species in biodiscovery programs.

INTRODUCTION

Bacterial infectious diseases are a major cause of death and morbidity worldwide.¹ The availability of antibiotics has saved millions of lives over the last century,² but the widespread and irresponsible use of antibiotics in medicine, agriculture, and the food industry has increased selection pressure for the evolution of resistant microbial strains.^{1,3,4} The pace of adaptation in microbial communities far outstrips the rate at which novel antibiotics are discovered and approved. This ultimately threatens the future efficacy of antibiotics, and the World Health Organization classified antibiotic resistance as a leading threat to global health.¹ Accordingly, the identification of novel antibiotic leads, especially those effective against critical (WHO priority 1) and high-priority (WHO priority 2) pathogens such as *Pseudomonas aeruginosa* and methicillin-resistant *Staphylococcus aureus* (MRSA), is a major research objective.^{5,6} Most of the current antibiotics are natural products discovered in microbes,⁷ but the urgent need for fundamentally new leads requires broader sampling across taxonomic space.

One of the most promising sources of novel antimicrobial molecules are animal venoms.⁸ These are complex cocktails with hundreds to thousands of components that facilitate predation, defense, and intraspecific competition.^{9,10} The proteins and peptides found in venom are described as toxins and have been evolutionarily refined through millions of years of natural selection.¹¹ Venom toxins have thus acquired unprecedented target selectivity and potency, which has been exploited to develop drugs for the treatment of hypertension, pain, and type 2 diabetes.^{12–15} More recent investigations of venom toxins have also revealed potent anti-infective activities.^{8,13,16–20} Given that most venoms have yet to be investigated, they offer an important source of potential new anti-infective leads.²¹

Arachnids (spiders and their kin) are among the most diverse and speciose terrestrial animals, with 20-fold more species than venomous snakes, and therefore offer immense potential for biodiscovery. They also feature some of the chemically most complex venoms, containing up to 3,000 toxins.²² Spider venoms are therefore predicted to yield at least 10 million new biomolecules, and this number will only rise when more diverse arachnid taxa are considered.¹⁴ Arachnid venoms also have unique pharmacological properties²³ because they have evolved to

¹Institute of Pharmaceutical Biology, Faculty of Biochemistry, Chemistry and Pharmacy, Goethe University Frankfurt, 60438 Frankfurt, Germany

²LOEWE Center for Translational Biodiversity Genomics (LOEWE-TBG), Senckenberganlage 25, 60325 Frankfurt, Germany

³Fraunhofer Institute for Translational Medicine and Pharmacology (ITMP), 60596 Frankfurt, Germany

⁴Branch of Bioresources, Fraunhofer Institute for Molecular Biology and Applied Ecology (IME-BR), 35392 Giessen, Germany

⁵Institute of Zoology, University of Cologne, Zulpicher Strasse 47b, 50674 Cologne, Germany

⁶Institute for Insect Biotechnology, Justus-Liebig-University of Giessen, Heinrich-Buff-Ring 26–32, 35392 Giessen, Germany

⁷German Center for Infection Research (DZIF), Partner Site Giessen-Marburg-Langen, Ohlebergsweg 12, 35392 Giessen, Germany

⁸Pharmaceutical Biology, Department of Pharmacy – Center for Drug Research, Ludwig-Maximilians-Universität München, Butenandtstr. 5-13, 81377 Munich, Germany

⁹These authors contributed equally

¹⁰Lead contact

*Correspondence: r.fuerst@lmu.de (R.F.), tim.lueddecke@ime.fraunhofer.de (T.L.)

<https://doi.org/10.1016/j.isci.2024.110209>



target insects and often display little to no toxicity against vertebrates, including humans.^{24,25} Furthermore, a significant proportion of arachnid toxins serves to prevent microbial colonization of the venom gland.^{19,26–28} This combination of chemical diversity and powerful pharmacology suggests that arachnids may be the most promising venom-based source of biomedical innovation, including the field of antimicrobial drugs.²⁹

Despite the promise of arachnid venoms, few toxins have been isolated and an even smaller number has been functionally characterized.^{21,30,31} This reflects an anthropocentric bias toward larger and potentially more dangerous species, especially those in which venom is easier to access. Thus far, venom biodiscovery has been largely activity guided, with crude venoms separated by chromatography before individual fractions are analyzed to determine toxin structure and function.³⁰ These strategies require milligram amounts of crude venom, which cannot be obtained from smaller arachnids representing the majority of species. Advances in mass spectrometry, next-generation sequencing, and biotechnology now enable a more holistic approach (venomics) to taxonomic sampling, followed by the production of selected toxins as synthetic or recombinant polypeptides in large amounts.^{32–34} For the first time, it is now possible to disentangle the venom composition of tiniest animals and study the function of any component for biomedical applications.

With respect to their venom composition, the pseudoscorpions are largely overlooked arachnids, and hence, their potential for biodiscovery of novel toxins is high.^{35,36} Locheiratan pseudoscorpions have a unique venom delivery system comprising pedipalps equipped with venom glands and specialized teeth, which grasp prey while the venom is injected.^{37,38} Pseudoscorpions tend to be small (most are only a few millimeters in length) and produce tiny amounts of venom, which has limited our ability to study them until recently.³⁹ A few studies have been carried out in the last 5 years, revealing the presence of several pharmacologically promising toxins.^{36,39,40} For example, the venom of the house pseudoscorpion (*Chelifer cancroides*) contains checacins, a novel family of toxins with eight known members (checacins 1 to 7 and the toxin referred to as Novel *Chelifer* Venom Compound 11 [NCVC 11]).³⁹ These are similar to meginin, a toxin from the Mediterranean checkered scorpion (*Mesobuthus gibbosus*) known to possess antimicrobial activity.^{39,41} An initial exploratory assessment of checacin 1, and some of its naturally occurring truncated derivatives, showed promising antibacterial effects.³⁵ Pseudoscorpions may therefore produce a large but hitherto unknown library of potential antimicrobial agents, but extensive bioactivity profiling is required for confirmation.

Here, we report the first *in silico* structural analysis and empirical functional characterization of the checacin family of pseudoscorpion toxins, including tests for activity against Gram-negative and Gram-positive bacterial pathogens and pathogenic fungi. We also tested their cytotoxicity against a range of cancer cell lines and primary cells and their ability to influence the release of calcium, nitrogen oxide (NO), and cyclic adenosine triphosphate (cAMP). Our work provides insight into the evolution of pseudoscorpion venom toxins and underpins the significance of the smallest arthropods for translational biodiscovery.

RESULTS

The sequence–structure space of checacins

Multiple sequence alignment revealed a high degree of sequence conservation among the eight known members of the checacin family, with the exception of the elongated N-terminal segment of checacin 6 (Figure 1). Molecular phylogenetic analysis showed that the checacins are monophyletic and that NCVC 11 is placed sister to all other checacins. Based on the phylogeny and the checacin's diagnostic C-terminus, we classified these peptides into two major groups. The first contains checacins 3 and 7, which have a conserved QAR motif, and the second contains checacins 1, 2, 4, 5, and 6, which have a conserved C-terminus containing 2–3 lysine residues. To these we refer as the QAR and KKK groups, respectively. The KKK group is subdivided into two clades, one composed by the checacins 1, 5, and 6 and the other containing checacins 2 and 4. The latter is placed sister to the QAR group peptides.

All checacins are predicted to be cationic, with sequence-based charges ranging from +2 to +7 and additional charges caused by C-terminal amidation (Table S1). They also feature alternating hydrophobic and hydrophilic amino acids, indicating the presence of membrane-interacting α -helical secondary structures that often confer antimicrobial activity (Figure 1).⁴² HeliQuest also predicted the formation of amphipathic helices (Figure 1, Table S1), although the helical signals were ambiguous for checacin 6. The antimicrobial peptide (AMP) calculator and predictor tool from AMP database v3 (Table S2)⁴³ reported high similarities to known AMPs, particularly those from amphibians but also arthropods and fish. Furthermore, AMP scanner vr.2 (which uses deep learning to predict antimicrobial activity based on a neural network trained on >1,700 known AMPs and the same number of non-AMPs)⁴⁴ also supported the predicted antimicrobial activity of all checacins, except checacin 6 (Table S1).

Checacins show potent activity against pathogenic bacteria

We determined the minimal inhibitory concentrations (MIC) of the checacins against six pathogenic microorganisms featuring a diverse panel of cell envelope architectures: the Gram-negative bacteria *Escherichia coli* and *Pseudomonas aeruginosa*, the Gram-positive bacteria *Mycobacterium smegmatis* (a surrogate for *Mycobacterium tuberculosis*) and MRSA, and the fungi *Aspergillus flavus* and *Candida albicans*.

All the checacins except checacin 6 were active against at least one bacterial strain, and some also showed antifungal activity (Table 1). *E. coli* was strongly inhibited by NCVC 11 (MIC <1.56 μ M) and moderately by checacin 5 (MIC = 3.25–6.25 μ M), whereas checacins 2 and 4 had a weaker effect. *P. aeruginosa* was strongly inhibited by NCVC 11 (MIC = 3.125–6.25 μ M), and was also inhibited to various degrees by checacins 1, 2, 4, and 5 but not by checacins 3, 6, and 7. *M. smegmatis* was inhibited only by NCVC 11 (MICs = 3.125 μ M), checacin 2 (MIC = 25–50 μ M), and checacin 5 (MIC = 12.5–25 μ M). All checacins except checacin 6 were active against MRSA, with checacins 2, 4, 5, and NCVC 11 achieving MICs of 1.56–3.125 μ M but lower values for checacin 7 (MIC = 3.125–6.25 μ M) and checacin 3 (MIC = 12.5–25 μ M). None of the peptides showed activity against *A. flavus*, but *C. albicans* was inhibited by checacins 4 (MIC = 6.25–12.5 μ M), 5

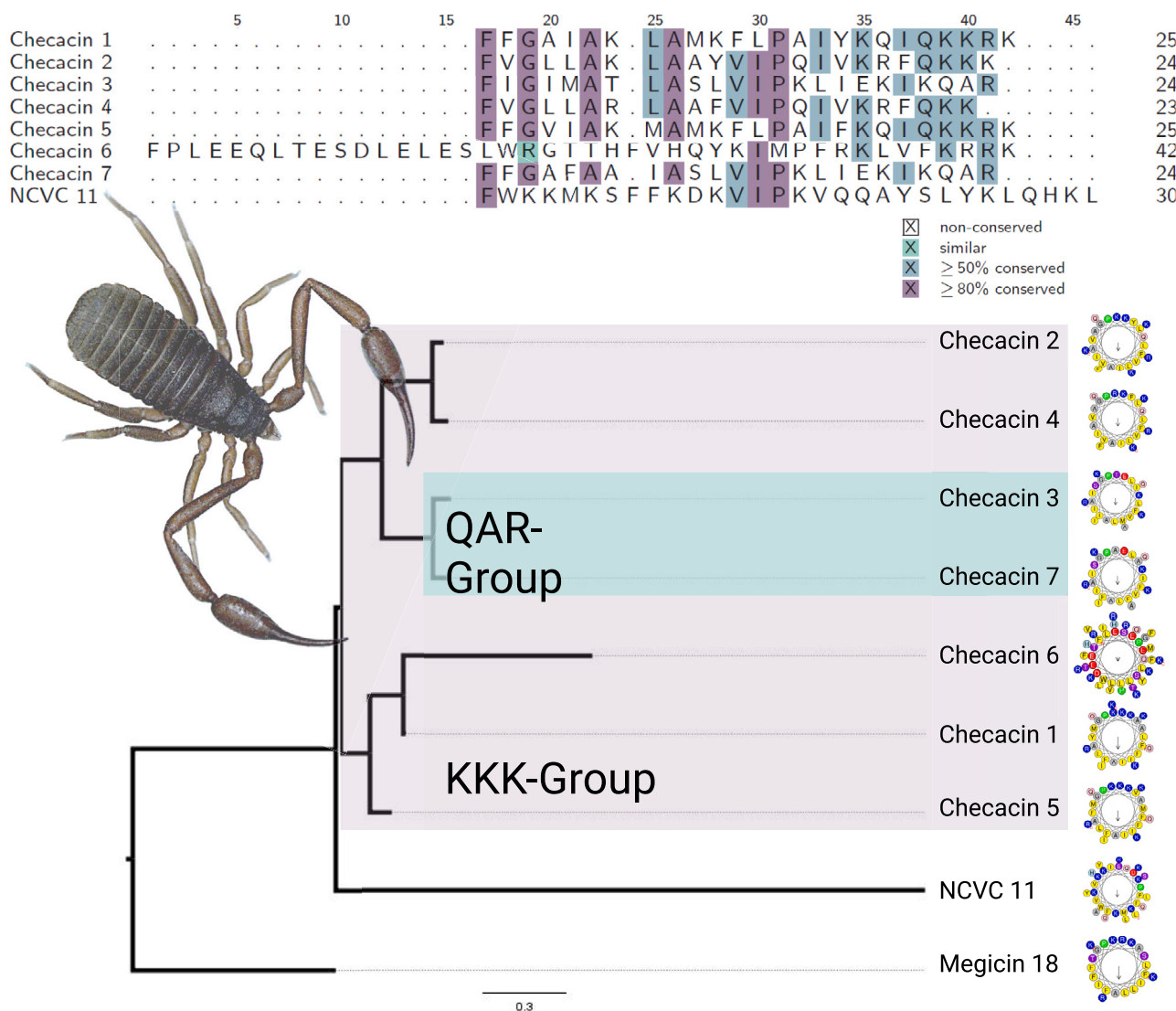


Figure 1. Sequence–structure space of the checacin family

Top: multiple sequence alignment of known checacins. Bottom: phylogenetic tree of all known checacins rooted by using the related scorpion toxin meginin 18 as an outgroup and calculated using IQ-TREE. Members of the KKK group are highlighted in purple, whereas members of the QAR group are highlighted in green. Helical wheel projections were calculated using HeliQuest. Hydrophobic residues are highlighted in yellow, and arrows indicate the site and direction of the hydrophobic moment.

(MIC = 12.5 μ M), and 2 (MIC = 12.5–25 μ M). The activities of checacins against Gram-negative bacteria (*E. coli* and *P. aeruginosa*) and MRSA were promising, and NCVC 11 repeatedly showed the most potent growth inhibition at low micromolar concentrations (MIC <6.25 μ M in *P. aeruginosa* and 0.8–0.4 μ M in *E. coli*).

Checacins show cell-type-dependent cytotoxic and anti-proliferative effects

We initially tested the cytotoxicity of checacins against human embryonic kidney 293 (HEK293T) and murine monocyte/macrophage-like (RAW264.7) cells (Figure 2). Cell viability was assessed by spectrophotometry following a formazan-based assay. At the highest concentration (25 μ g/mL), all checacins except checacin 6 and NCVC 11 reduced the viability of both cell lines, whereas checacin 6 and NCVC 11 had no effect. We also investigated the effects of the naturally occurring truncated checacin 1 derivatives checacin 1^{1–21}, checacin 1^{1–11}, and checacin 1^{12–25}. The longest derivative (checacin 1^{1–21}) reduced the viability of both cell lines, but the shorter ones did not, suggesting that the shorter derivatives lack specific cytotoxic motifs.

We also assessed the ability of checacins to inhibit the proliferation of sub-confluent primary human umbilical vein endothelial cells (HUVECs) and primary normal human dermal fibroblasts (NHDFs), as well as the cancer cell lines HeLa and MDA-MB-231, using a crystal violet

Table 1. Antimicrobial activity of checacins based on minimum inhibitory concentrations (MIC/ μ M) including previously determined values for checacin 1 and its derivatives

Peptide	<i>E. coli</i> ATCC35218	<i>P. aeruginosa</i> ATCC27853	<i>M. smegmatis</i> ATCC607	<i>S. aureus</i> (MRSA) ATCC33592	<i>A. flavus</i> ATCC9170	<i>C. albicans</i> FH2173
Checacin 1 ^a	1.6–0.8 (1.6)	12.5	25	1.56	50	6.25
Checacin 1 ^{1–11a}	>50 (>50)	>50	>50	>50	>50	>50
Checacin 1 ^{12–25a}	>50 (>50)	>50	>50	>50	>50	>50
Checacin 1 ^{1–21a}	>50 (>50)	>50	>50	12.5	>50	>50
Checacin 2	12.5–6.25 (3.125)	12.5–6.25	50–25	1.56	>50	25–12.5
Checacin 3	>50 (50)	>50	>50	25–12.5	>50	50
Checacin 4	25–12.5 (6.25)	25	50	3.125–1.56	>50	12.5–6.25
Checacin 5	6.25 (3.25)	12.5–6.25	25–12.5	3.125–1.56	>50	12.5
Checacin 6	>50 (>50)	>50	>50	>50	>50	>50
Checacin 7	>50 (>50)	>50	>50	6.25–3.125	>50	>50
NCVC 11	1.56 (0.8–0.4)	6.25–3.125	3.125	3.125–1.56	>50	>50

Activities were measured against different bacteria and fungi on MHII and MHC (in brackets) media.

^aData from Krämer et al.³⁵

assay (Figure 3). Checacin 1 and checacin 1^{1–21} only affected cancer cells at the highest concentration (25 μ g/mL), and checacin 1 also inhibited the proliferation of NHDFs. Conversely, checacin 1^{1–11} and checacin 1^{12–25} had only a marginal effect on the proliferation of healthy cells. All other peptides except checacin 6 inhibited the proliferation of cancer cells at the highest concentration (25 μ g/mL), and five peptides (checacin 1, checacin 1^{1–21}, checacin 3, checacin 7, and NCVC 11) also inhibited the proliferation of healthy cells (Figure 3A). We tested three additional concentrations (2.5–25 μ g/mL) of each peptide, which revealed that NCVC 11 inhibited the proliferation of HeLa (5–15 μ g/mL) and MDA-MB-231 (15 μ g/mL) cancer cells without affecting HUVECs or NHDFs (Figure 4).

Checacins induce Ca²⁺ release and inhibit cAMP signaling

To investigate the physiological effects of checacins, we measured the ability of cells to release Ca²⁺ and cyclic adenosine monophosphate (cAMP) following toxin exposure (Figure 5), given that these second messengers are induced by the activation of cell surface receptors and participate in key cellular functions, including muscle contraction and inflammation. Interestingly, exposure to most of the peptides (2.5 μ g/mL) increased intracellular Ca²⁺ levels, with checacin 1^{1–11}, checacin 1^{12–25}, and checacin 6 as the only exceptions (Figure 5A). When HEK293T cells were pre-incubated with these toxins, they did not inhibit Ca²⁺ release induced by ionomycin. None of the toxins induced cAMP release, but all except the checacin 1 derivatives and checacin 6 inhibited cAMP release induced by forskolin.

Checacins influence NO release *in vitro*

NO synthesized by inducible NO synthase (iNOS) in phagocytes is a component of the innate immune response to pathogens. Accordingly, we investigated the ability of checacins to influence NO synthesis in RAW264.7 macrophages (Figure 6). We found that none of the checacins induced NO synthesis but all except the checacin 1 derivatives inhibited NO synthesis at a concentration of 2.5 μ g/mL. Our data therefore suggest that checacins have a direct anti-pathogenic effect but simultaneously interfere with the anti-pathogenic function of phagocytes.

DISCUSSION

Checacins highlight the significance of small arthropods for venom biodiscovery

Animal venoms are a rich source of new drug leads, with several already approved such as Captopril, Ziconotide, and Exenatide.¹³ However, anthropocentric bias and methodological restrictions have restricted the scope to a non-representative group of venomous animals,²¹ mostly excluding small arthropod lineages despite their astounding diversity.²² In the present study, we have used information on the presence and structures of checacins recently discovered in one of these arthropod groups, the pseudoscorpions, to perform a comprehensive bioactivity profiling of the multiple checacins. Most of the checacins feature structural motifs that suggest antimicrobial activity, and this was confirmed in our *in vitro* functional assays. In our initial evaluation, most checacins inhibited the growth of clinically relevant bacterial pathogens. Some checacins inhibited the growth of Gram-negative as well as Gram-positive bacteria. Interestingly, compound NCVC11 inhibited the growth of the critical priority bacteria *Pseudomonas aeruginosa* and *E. coli* (1.56–6.25 μ M) without inhibiting human embryonic kidney and murine monocyte/macrophage-like cells at 25 μ g/mL. Due to the cationic nature of this group of toxins, further studies should investigate whether strains with lipid-A-modifying resistance mechanisms, such as MCR-1 expression, exhibit the same degree of susceptibility. In that sense, colistin resistance development and/or cross-resistance as a consequence of toxin exposure should be analyzed.⁴⁵ With the exception of the atypical checacin 6, all other full-length checacins (particularly the KKK group) and even the truncated derivative checacin 1^{1–21} inhibited

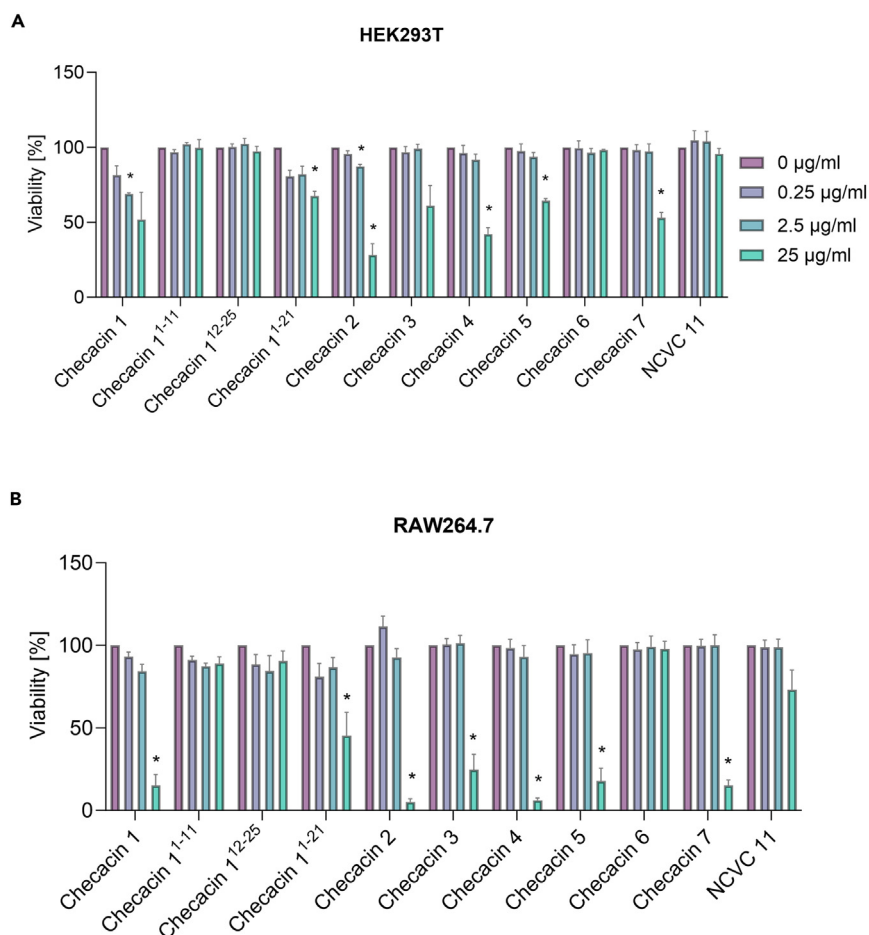


Figure 2. Effects of checacins on cell viability

(A) HEK293T and (B) RAW264.7 cells were treated with checacins at the indicated concentrations for 24 h, followed by incubation with WST-8. The formation of formazan was detected by absorbance spectrophotometry. Viability was calculated as the absorbance relative to control samples. Data are means \pm SEM ($n = 3$, $*p \leq 0.05$ vs. control).

the growth of MRSA, some at concentrations as low as 1.56 μM . Furthermore, the KKK checacins also displayed moderate activity against *C. albicans*, suggesting additional potential as an anti-fungal. However, checacins with antimicrobial effects also tended to be cytotoxic, reducing the viability of primary human cells and influencing cell signaling and NO synthesis. This suggests the potential for side effects, and further engineering may therefore be required before lead development.⁴⁶ Checacins 1, 2, 4, 5, and NCVC11 showed potent activity against cancer cell lines, but clarifying their suitability as anticancer components demands further investigations.

The activity profile of checacins further highlights the importance of including neglected lineages in venom biodiscovery programs. The house pseudoscorpion produces eight checacins, seven showing antimicrobial activity.^{35,39,40} Extrapolating this to the entire family of Cheliferidae, which features more than 60 genera and at least 270 species, results in a high number of promising molecules to be investigated, assuming that a similar number of checacins can be found in the venom of all species.³⁹ The same principle applies to the multitude of small spiders, scorpions, and ticks that are likewise known to produce toxins with potent antimicrobial activities but have yet to be investigated.^{19,26,31,47} However, many arthropods may fall victim to the global biodiversity crisis, due to environmental destruction and declining prey populations.^{48–50} To avoid losing the treasure trove of bioactive compounds in animal venoms, biodiversity preservation should be combined with venom surveys to preserve and catalog these promising lineages.

Structural insights into checacin bioactivity

Our analysis of the checacins included an assessment of the sequence–structure space using a variety of *in silico* approaches, which we combined with our *in vitro* data to draw several inferences about the structure–function relationship in this family. With the exception of checacin 6, the KKK checacins appeared to show the most potent activity against bacteria and were the only peptides to affect fungi. The presence of multiple (in NCVC 11 one) lysine residues, which makes these peptides cationic, facilitates the attraction toward negatively charged lipid

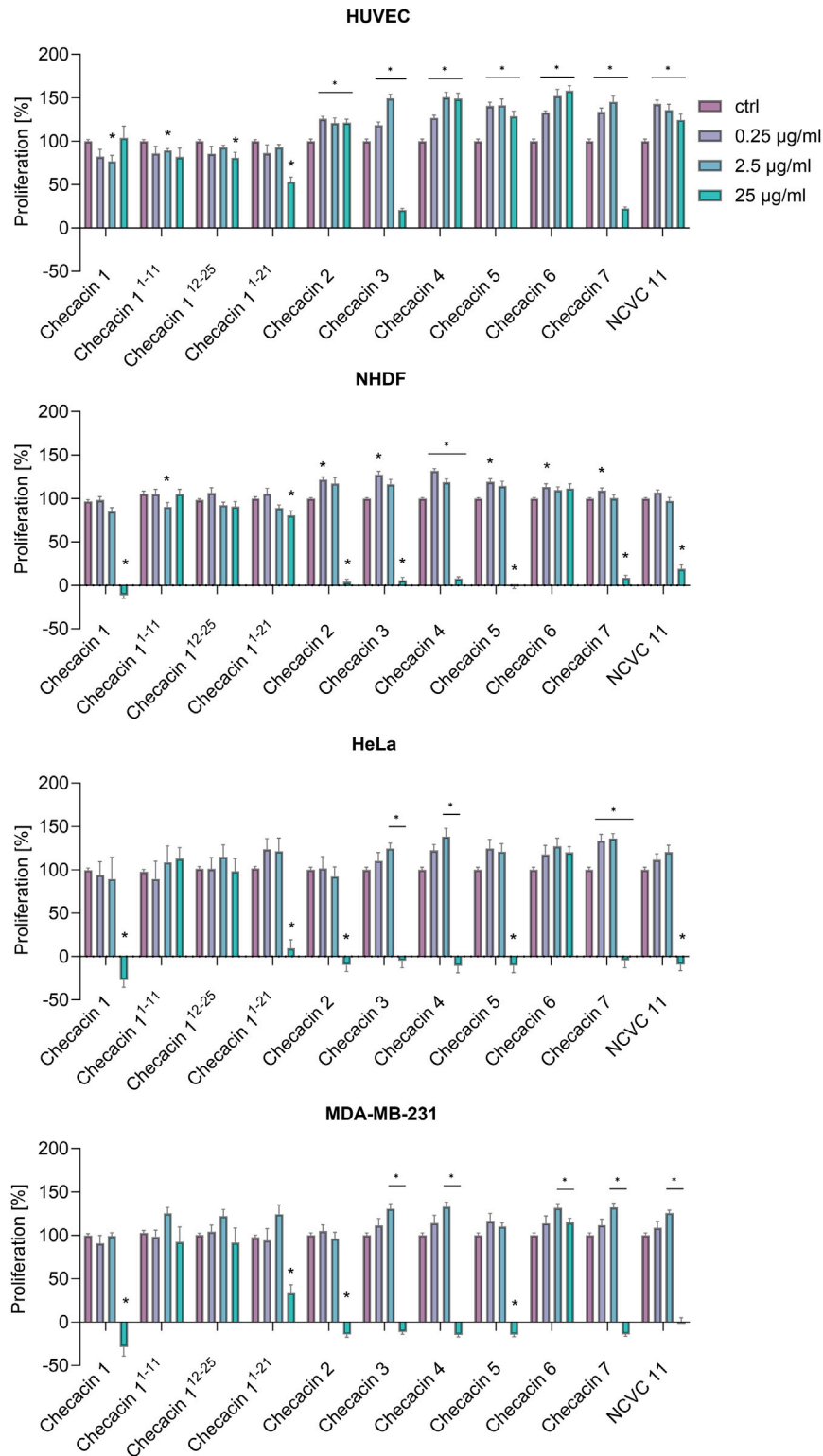


Figure 3. The ability of checacins to inhibit the proliferation of healthy primary cells and cancer cell lines

All cells were grown at low density for 24 h before treatment with 0.25, 2.5, and 25 µg/mL of each peptide. Cells were stained with a crystal violet after 72 h, and the amount of DNA-bound crystal violet was detected by spectrophotometry. Data are means \pm SEM ($n = 3$, $*p \leq 0.05$ vs. control).

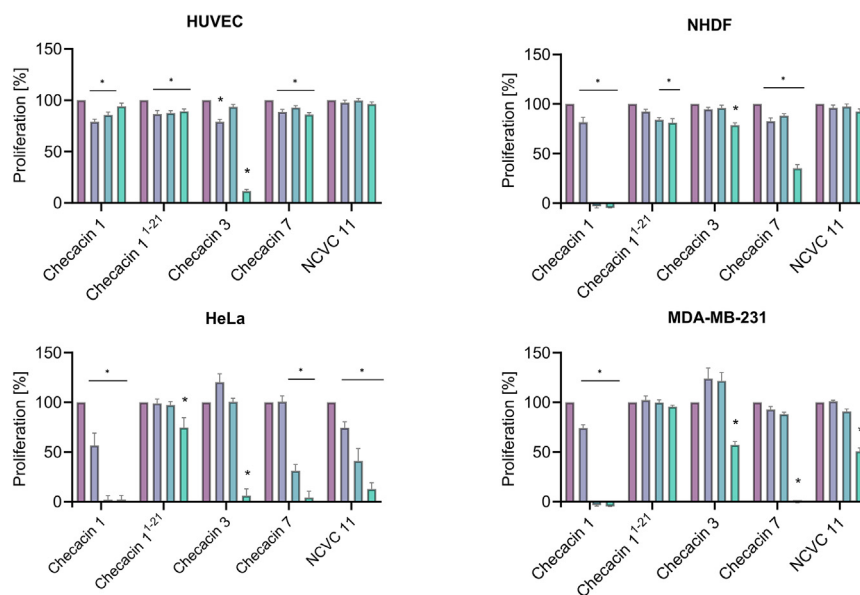


Figure 4. Effects of low concentrations of Checacin toxins on proliferation

All cells were grown in low density for 24 h before treatment with 5, 10, and 15 μg/mL concentrations of each component. Cells were stained with a crystal violet solution after 72 h, and the amount of DNA-bound crystal violet was detected photometrically. Data are expressed as mean ± SEM. $n = 3$ * $p \leq 0.05$ vs. control.

bilayers of biomembranes.⁵¹ Interestingly, the lysine-rich checacins also showed the highest diversity, suggesting their biological significance exceeds that of the other lineages. Full-length checacin 1 and its derivative checacin 1¹⁻²¹ (lacking the C-terminal lysine-rich motif) showed potent cytotoxic effects and influenced the release of second messengers, suggesting the lysine-rich motif is not required for this property. Interestingly, checacin 1¹⁻¹¹ and 1¹²⁻²⁵ (consisting of the first 11 and last 14 amino acids, respectively) showed no effects in these assays, possibly reflecting their lower net charge and hydrophobicity compared to full-length checacin 1 and checacin 1¹⁻²¹. Our data also indicate that the effects of checacin 1 and checacin 1¹⁻²¹ may require a secondary structure that is absent in the other truncated derivatives. The release of second messengers is mainly driven by the activation of cell surface receptors, which supports the hypothesis that the structure of checacin 1 derivatives is relevant to the observed effects.⁵²

Checacins 3 and 7 (QAR group) strongly inhibited the proliferation of HUVECs, possibly due to the C-terminal arginine residue, given that arginine is associated with the production of NO in endothelial cells. However, once the NO synthesis machinery is saturated, further arginine uptake is usually accompanied by the production of toxic superoxide.⁵³ It is therefore necessary to balance NO production to ensure the beneficial effects without oxidative stress or endothelial dysfunction. Lower concentrations of QAR checacins had no significant effect on HUVECs.

The biological role of checacin toxins

Our work also allows us to postulate novel hypotheses upon the evolution and ecology of arachnid venoms.²¹ We found that many of the tested checacins are multifunctional, with both antimicrobial and cytotoxic effects. Pseudoscorpions generally use venom in a trophic context to overpower other arthropods.³⁹ Their venom contains several putative neurotoxic peptides that probably interfere with voltage-gated potassium and sodium channels.^{29,40,54} Trophic venom must induce rapid effects to ensure immediate prey paralysis, and these neurotoxic peptides are likely to fulfill such a function. In contrast, checacin 1 and its derivatives showed insecticidal activity in aphid feeding assays, but only after 72 h.³⁵ This makes a trophic role for checacins unlikely, although feeding assays do not provide clear insight into the biological roles of injected toxins. Notably, pea aphids have evolved an obligate form of nutritional symbiosis with the bacterium *Buchnera aphidicola*,⁵⁵ so the insecticidal effect of checacins during feeding assays may be indirect, resulting from antimicrobial or cytotoxic activity against the vital symbionts. A similar mode of action has previously been reported for orally applied aphicidal scorpion toxins.⁵⁶

First assumptions about the biological role of checacins can be made based on previous insights on similar toxins across the metazoan Tree of Life. Several checacins are similar to toxins from amphibian skin poisons, which are also multifunctional with potent antimicrobial and cytotoxic activity.^{57,58} Like pseudoscorpion venom, amphibian skin poison is a complex mixture of neurotoxins and antimicrobial toxins.⁵⁹⁻⁶² The cytotoxic effects of amphibian skin poison increase the uptake of cosecreted neurotoxins into the victim, thereby increasing the overall toxicity of the secretion.⁶³ Amphibian antimicrobial toxins are therefore not only a defense against microbial infection but also synergistic enhancers of neurotoxic activity.^{57,63} We propose that checacins and amphibian toxins have a similar set of functions, facilitating the defense of the venom gland against pathogens as well as the enhancement of toxicity in trophic scenarios. The defense hypothesis is supported by venom microbiome analysis.⁶⁴ Contrary to past assumptions of sterility, venom is now known to be colonized by bacteria.⁶⁵⁻⁶⁸

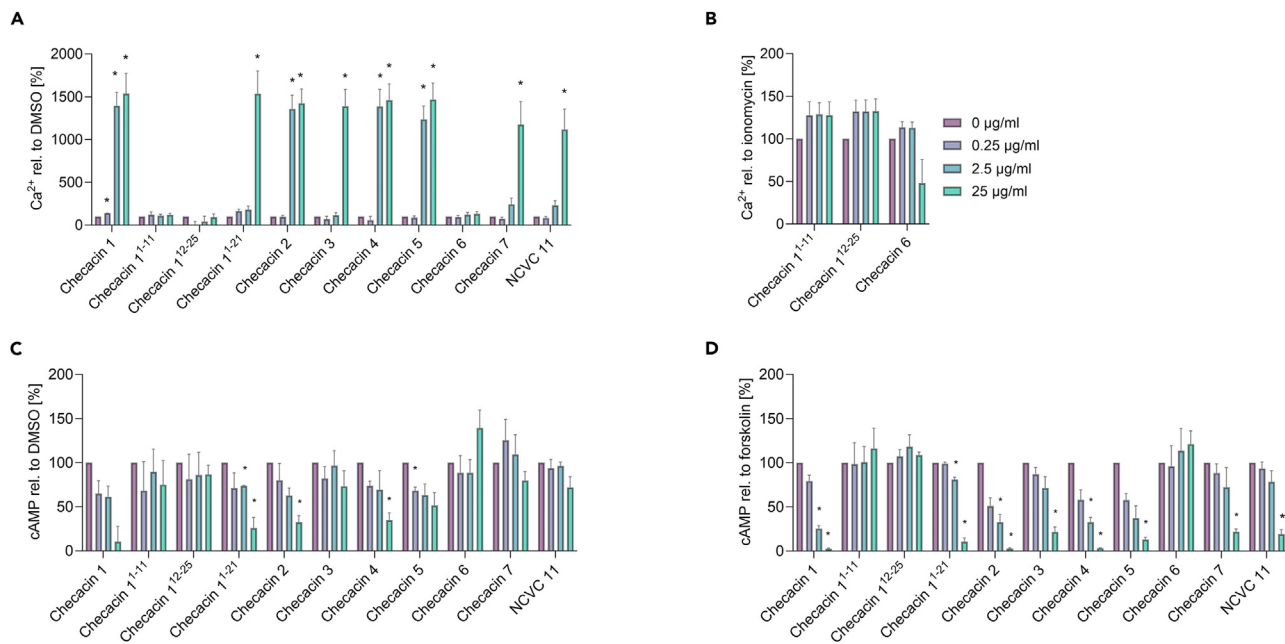


Figure 5. Checacins influence the release of second messengers

(A and B) Effects on the release of Ca²⁺: (A) Fluo-8 pre-treated HEK293T cells were incubated with checacins at the indicated concentrations followed by fluorescence analysis to detect intracellular Ca²⁺; (B) Fluo-8 pre-treated HEK293T incubated with peptides at the indicated concentrations for 30 min were stimulated with 5 µM ionomycin followed by fluorescence analysis to detect intracellular Ca²⁺. (C and D) Effects on the release of cAMP: (C) HEK293T cells transfected with pGloSensor-22F were treated with checacins (0.25, 2.5, and 25 µg/mL) in the presence of the pGloSensor cAMP reagent, followed by luminescence analysis to detect cAMP; (D) HEK293T cells transfected with pGloSensor-22F were treated with checacins (0.25, 2.5, and 25 µg/mL) in the presence of the pGloSensor cAMP reagent and 5 µM forskolin, followed by luminescence analysis to detect cAMP. Data are means ± SEM (n = 3, *p ≤ 0.05 vs. control).

Given the enlarged lumen of venom glands and the nutrient-rich composition of venom, microbial infection of venom glands could pose a risk to predators. Hence, the recruitment of antimicrobial components would help to either control such microbial communities or defend against infection. Interestingly, α-helical antimicrobial toxins are not present solely in spider venom but widely across arthropods and particularly arachnids.^{17,61,69,70} This supports the hypothesis that plesiotypic antimicrobial toxins were recruited to defend against microbial infection but evolved toward today's apotypic multifunctionality according to the same mechanism as known from amphibians.^{56,63} The weaponization of innate immune system components into the chemical arsenal of venom systems appears to be a successful strategy, given the diverse animal lineages in which this phenomenon has arisen by convergent evolution.

The expression levels of checacins and the relative intensities of their signals in mass spectra of the venom of *C. cancrivora* are surprisingly different.⁴⁰ This raises the question whether a relationship between their concentration in the venom and the efficacy determined in our study exists. Theoretically possible seems to be both upregulation of gene expression at lower efficacy and downregulation of gene expression at low efficacy, simply to save energy. Our tests show a rather mixed picture. As illustrated in Figure 1, based on their nucleotide sequences, the eight checacins precursors can be classified into two groups. Presumably, these groups reflect the evolution of the checacins genes by gene duplications in *C. cancrivora*. It appears that the various members of the KKK group represent the more plesiotypic toxins within the checacins family and that QAR group peptides evolved from them (Figure 1). Interestingly, KKK group member checacins 6 and the toxin NVCV 11, which is placed sister to all other checacins, were both detected with lower relative intensities in mass spectra of the venom when compared to the other checacins.⁴⁰ While checacins 6 did not show significant efficacy in our bioassays, NVCV 11 was highly effective against bacteria. This cannot be interpreted conclusively with our current knowledge. However, for the other checacins, there is a clear correlation between the relative intensities in mass spectra of the venom and the efficacy in our tests on microbes. The paracopies that tend to be less effective against bacteria (checacins 3, 4, 7) are only slightly accumulated in the venom, whereas the paracopies that were more effective in our tests (checacins 1, 2, 5) are more highly accumulated. Checacins 1 is clearly the most effective peptide of this group (Table 1) and is also the most enriched in the venom.⁴⁰

Conclusion and future perspectives

Animal venoms offer a promising source of novel biomolecules with translational potential in biomedicine and agriculture, but few taxa have been analyzed in detail, especially in terms of function. This is especially true for small arthropod lineages, where a large number of potent biomolecular innovations are awaiting discovery. We have presented the first functional investigation of all known checacins. These are major

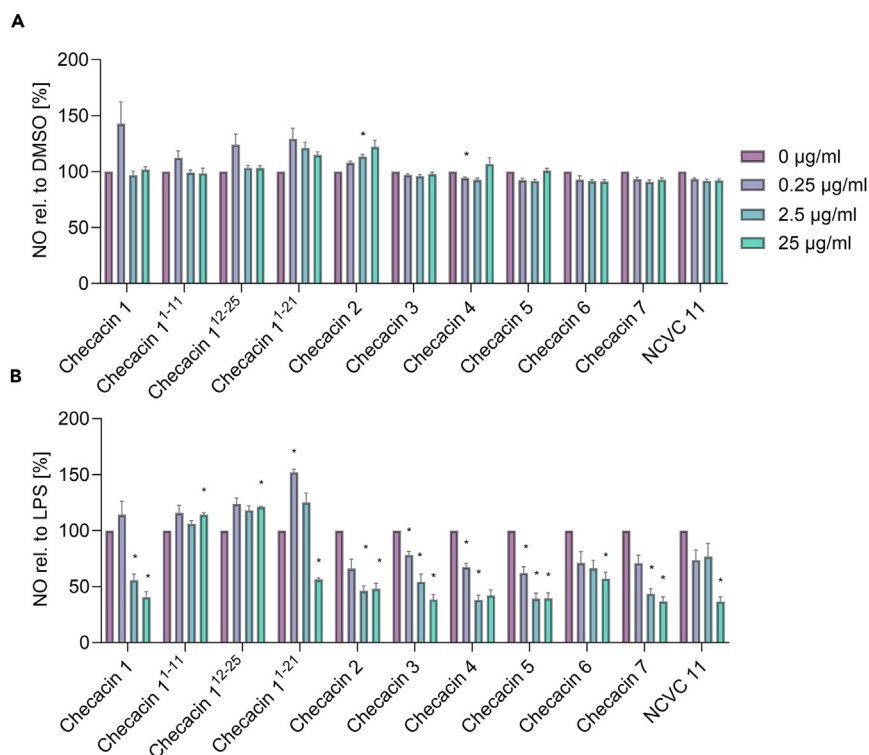


Figure 6. Influence of checacins on inflammation-associated cell functions

(A) RAW264.7 cells were treated with checacins for 24 h before screening for the enhanced production of NO.

(B) RAW264.7 cells were pretreated for 30 min and then stimulated with 100 ng/mL LPS for 24 h before screening for the inhibition of NO production. NO was detected in the supernatant using the Griess method. Data are means \pm SEM ($n = 3$, $*p \leq 0.05$ vs. control).

venom components of the pseudoscorpion *C. cancroides*, representing a group of venomous animals that has been largely overlooked. Our experiments revealed that several checacins inhibit the growth of Gram-negative bacteria and MRSA but also interfere with the proliferation and signaling capacity of human cells, which could lead to side effects. However, the engineering of these could yield recombinant or synthetic derivatives with more potent antimicrobial activity and fewer detrimental effects in humans. The array of checacins discovered thus far stems only from a single pseudoscorpion species among hundreds that remain to be investigated. Venomic surveys across pseudoscorpions are therefore needed to exploit the diversity of checacins and thereby deliver more promising molecules. Based on our activity data, we postulate novel hypotheses on the evolutionary ecology of checacins. We hypothesize that they probably arose as antimicrobial defenders of the venom gland and that apotypic descendants subsequently evolved toward an additional role of spreading factors for the venom cocktail. A deeper understanding of pseudoscorpion venom evolution would require the testing of a larger array of toxins in concert with pseudoscorpion genome analysis. On a larger scale, our work delivers proof of concept highlighting the importance of the smallest, most neglected arthropods for venom biodiscovery. It shows that even the tiniest animals have the potential for discovering highly promising compounds that could ultimately yield new drug leads for the benefit of humans.

Limitations of the study

In this work, we shed light on the bioactivity profile of linear pseudoscorpion toxins from the checacins family. Although our work adds important novel insights into the translational potential and biological role of toxins from some of Earth's least studied venomous animals, it may be limited for several reasons. First, the taxonomic limitations for sourcing checacins for profiling and selecting model systems for bioassays may play a role here. On one hand, all checacins herein chosen are derived from *C. cancroides*, a single member of pseudoscorpions. Future works should investigate more pseudoscorpion venoms to identify additional checacins, which in turn could add important insights to better integrate our findings in context of a wider selection of toxins. Similarly, the restriction to selected bacterial and mammalian model systems for bioassays may influence the conclusions drawn. Especially, future works should aim to include rigorously controlled *in vivo* experiments to validate our conclusions. Lastly, arachnid toxins are known to often exert synergistic activities, and thus combinatorial assays may be required to fully unveil the bioactivity spectrum of arachnid toxins.²⁹ As of yet, this aspect is fully unstudied for pseudoscorpion toxins, and future works should perform bioactivity assays with combinations of checacins.

STAR★METHODS

Detailed methods are provided in the online version of this paper and include the following:

- **KEY RESOURCES TABLE**
- **RESOURCE AVAILABILITY**
 - Lead contact
 - Materials availability
 - Data and code availability
- **METHOD DETAILS**
 - Checacins
 - *In silico* analysis
 - Molecular phylogeny
 - Antimicrobial activity
 - Cells and reagents
 - Cell viability assay
 - Cell proliferation assay
 - Analysis of intracellular Ca²⁺ levels
 - Analysis of cAMP levels
 - Analysis of NO levels
- **QUANTIFICATION AND STATISTICAL ANALYSIS**

SUPPLEMENTAL INFORMATION

Supplemental information can be found online at <https://doi.org/10.1016/j.isci.2024.110209>.

ACKNOWLEDGMENTS

We thank Mareike Lang, Isabelle Petith and Kirsten Susann Bommersheim for technical assistance and Richard M. Twyman for valuable comments on this manuscript. All Figures were created using BioRender.

Funding: This work was financially supported by the Hessian Ministry of Science, Research and the Arts (HMWK) via the LOEWE Center for Translational Biodiversity Genomics (LOEWE-TBG) granted to A.V., S.S., and R.F., the LOEWE Research Centre for Novel Drug Targets against Poverty-Related and Neglected Tropical Infectious Diseases (DRUID, project E6 for S.S.), the Fraunhofer Cluster of Excellence Immune-Mediated Diseases (CIMD), and the Leistungszentrum Innovative Therapeutics (TheraNova).

AUTHOR CONTRIBUTIONS

Conceptualization, P.E., S.S., A.V., R.F. and T.L.; Methodology, P.E., S.S., T.U., M.H., M.M., and J.K.; Investigation, P.E., S.S., T.U., M.H., M.M., J.K., R.P., T.F.S., S.H., L.D., A.V., R.F., and T.L.; Formal analysis, P.E., S.S., M.M. R.F. and T.L.; Resources, R.P., T.F.S., A.V., R.F. and T.L.; Data curation, S.H., L.D. and T.L.; Writing - original draft, P.E., S.S., R.F. and T.L.; Writing - review and editing, T.U., M.H., M.M., J.K., R.P., T.F.S., S.H., L.D., and A.V.; Visualization, P.E., S.S., S.H., L.D. and T.L.; Supervision, S.S., R.P., T.F.S., A.V., R.F., and T.L.; Funding acquisition, S.S., A.V. and R.F.

DECLARATION OF INTERESTS

The authors declare no competing interests.

Received: January 27, 2024

Revised: April 24, 2024

Accepted: June 4, 2024

Published: June 8, 2024

REFERENCES

1. Ventola, C.L. (2015). The antibiotic resistance crisis: part 1: causes and threats. *Pharm. Therapeut.* *40*, 277–283. <https://doi.org/10.1016/j.mib.2019.10.008>
2. Hutchings, M.I., Truman, A.W., and Wilkinson, B. (2019). Antibiotics: past, present and future. *Curr. Opin. Microbiol.* *51*, 72–80. <https://doi.org/10.1016/j.mib.2019.10.008>
3. Davies, J., and Davies, D. (2010). Origins and evolution of antibiotic resistance. *Microbiol. Mol. Biol. Rev.* *74*, 417–433. <https://doi.org/10.1128/MMBR.00016-10>
4. Larsson, D.G.J., and Flach, C.-F. (2022). Antibiotic resistance in the environment. *Nat. Rev. Microbiol.* *20*, 257–269. <https://doi.org/10.1038/s41579-021-00649-x>
5. Vestergaard, M., Frees, D., and Ingmer, H. (2019). Antibiotic Resistance and the MRSA Problem. *Microbiol. Spectr.* *7*, 10–1128. <https://doi.org/10.1128/microbiolspec.GPP3-0057-2018>
6. Pang, Z., Raudonis, R., Glick, B.R., Lin, T.-J., and Cheng, Z. (2019). Antibiotic resistance in *Pseudomonas aeruginosa*: mechanisms and alternative therapeutic strategies. *Biotechnol. Adv.* *37*, 177–192. <https://doi.org/10.1016/j.biotechadv.2018.11.013>

7. Bérday, J. (2012). Thoughts and facts about antibiotics: where we are now and where we are heading. *J. Antibiot.* 65, 385–395. <https://doi.org/10.1038/ja.2012.27>.
8. Perumal Samy, R., Stiles, B.G., Franco, O.L., Sethi, G., and Lim, L.H.K. (2017). Animal venoms as antimicrobial agents. *Biochem. Pharmacol.* 134, 127–138. <https://doi.org/10.1016/j.bcp.2017.03.005>.
9. Casewell, N.R., Wüster, W., Vonk, F.J., Harrison, R.A., and Fry, B.G. (2013). Complex cocktails: the evolutionary novelty of venoms. *Trends Ecol. Evol.* 28, 219–229. <https://doi.org/10.1016/j.tree.2012.10.020>.
10. Schendel, V., Rash, L.D., Jenner, R.A., and Undheim, E.A.B. (2019). The Diversity of Venom: The Importance of Behavior and Venom System Morphology in Understanding Its Ecology and Evolution. *Toxins* 11, 666. <https://doi.org/10.3390/toxins11110666>.
11. Fry, B.G., Roelants, K., Champagne, D.E., Scheib, H., Tyndall, J.D.A., King, G.F., Nevalainen, T.J., Norman, J.A., Lewis, R.J., Norton, R.S., et al. (2009). The Toxicogenomic Multiverse: Recruitment of Proteins Into Animal Venoms. *Annu. Rev. Genomics Hum. Genet.* 10, 483–511. <https://doi.org/10.1146/annurev.genom.9.081307.164356>.
12. Estrada, G., Villegas, E., and Corzo, G. (2007). Spider venoms: a rich source of acylpolyamines and peptides as new leads for CNS drugs. *Nat. Prod. Rep.* 24, 145–161. <https://doi.org/10.1039/B603083C>.
13. Herzig, V., Cristofori-Armstrong, B., Israel, M.R., Nixon, S.A., Vetter, L., and King, G.F. (2020). Animal toxins - Nature's evolutionary-refined toolkit for basic research and drug discovery. *Biochem. Pharmacol.* 181, 114096. <https://doi.org/10.1016/j.bcp.2020.114096>.
14. Saez, N.J., Senff, S., Jensen, J.E., Er, S.Y., Herzig, V., Rash, L.D., and King, G.F. (2010). Spider-venom peptides as therapeutics. *Toxins* 2, 2851–2871. <https://doi.org/10.3390/toxins2122851>.
15. Dutertre, S., Undheim, E., PINEDA, S., Jin, A.-H., Lewis, R., Alewood, P., and King, G. (2015). Venoms-Based Drug Discovery: Proteomic and Transcriptomic Approaches (RSC Drug Discovery Series), pp. 80–96. <https://doi.org/10.1039/9781849737876-00080>.
16. Budnik, B.A., Olsen, J.V., Egorov, T.A., Anisimova, V.E., Galkina, T.G., Musolyamov, A.K., Grishin, E.V., and Zubarev, R.A. (2004). De novo sequencing of antimicrobial peptides isolated from the venom glands of the wolf spider *Lycosa singoriensis*. *J. Mass Spectrom.* 39, 193–201. <https://doi.org/10.1002/jms.577>.
17. Choi, J.H., Jang, A.Y., Lin, S., Lim, S., Kim, D., Park, K., Han, S.-M., Yeo, J.-H., and Seo, H.S. (2015). Melittin, a honeybee venom-derived antimicrobial peptide, may target methicillin-resistant *Staphylococcus aureus*. *Mol. Med. Rep.* 12, 6483–6490. <https://doi.org/10.3892/mmr.2015.4275>.
18. Hurka, S., Lüddecke, T., Paas, A., Dersch, L., Schulte, L., Eichberg, J., Hards, K., Brinkroff, K., and Vilcinskis, A. (2022). Bioactivity Profiling of In Silico Predicted Linear Toxins from the Ants *Myrmica rubra* and *Myrmica ruginodis*. *Toxins* 14, 846. <https://doi.org/10.3390/toxins14120846>.
19. Lüddecke, T., Dersch, L., Schulte, L., Hurka, S., Paas, A., Oberpaul, M., Eichberg, J., Hards, K., Klimpel, S., and Vilcinskis, A. (2023). Functional Profiling of the A-Family of Venom Peptides from the Wolf Spider *Lycosa shansia*. *Toxins* 15, 303. <https://doi.org/10.3390/toxins15050303>.
20. Eichberg, J., Maiworm, E., Oberpaul, M., Czudai-Matwich, V., Lüddecke, T., Vilcinskis, A., and Hards, K. (2022). Antiviral Potential of Natural Resources against Influenza Virus Infections. *Viruses* 14, 2452. <https://doi.org/10.3390/v14112452>.
21. von Reumont, B.M., Campbell, L.I., and Jenner, R.A. (2014). Quo vadis venomics? A roadmap to neglected venomous invertebrates. *Toxins* 6, 3488–3551. <https://doi.org/10.3390/toxins6123488>.
22. Pineda, S.S., Chin, Y.K.-Y., Undheim, E.A.B., Senff, S., Mobli, M., Dauly, C., Escoubas, P., Nicholson, G.M., Kaas, Q., Guo, S., et al. (2020). Structural venomics reveals evolution of a complex venom by duplication and diversification of an ancient peptide-encoding gene. *Proc. Natl. Acad. Sci. USA* 117, 11399–11408. <https://doi.org/10.1073/pnas.1914536117>.
23. Saez, N.J., and Herzig, V. (2019). Versatile spider venom peptides and their medical and agricultural applications. *Toxicon* 158, 109–126. <https://doi.org/10.1016/j.toxicon.2018.11.298>.
24. Windley, M.J., Herzig, V., Dziemborowicz, S.A., Hardy, M.C., King, G.F., and Nicholson, G.M. (2012). Spider-venom peptides as bioinsecticides. *Toxins* 4, 191–227. <https://doi.org/10.3390/toxins4030191>.
25. King, G.F., and Hardy, M.C. (2013). Spider-Venom Peptides: Structure, Pharmacology, and Potential for Control of Insect Pests. *Annu. Rev. Entomol.* 58, 475–496. <https://doi.org/10.1146/annurev-ento-120811-153650>.
26. Tang, X., Yang, J., Duan, Z., Jiang, L., Liu, Z., and Liang, S. (2020). Molecular diversification of antimicrobial peptides from the wolf spider *Lycosa sinensis* venom based on peptidomic, transcriptomic, and bioinformatic analyses. *Acta Biochim. Biophys. Sin.* 52, 1274–1280. <https://doi.org/10.1093/abbs/gmaa107>.
27. Abreu, T.F., Sumitomo, B.N., Nishiyama, M.Y., Oliveira, U.C., Souza, G.H.M.F., Kitano, E.S., Zelanis, A., Serrano, S.M.T., Junqueira-de-Azevedo, I., Silva, P.I., and Tashima, A.K. (2017). Peptidomics of *Acanthoscurria gomesiana* spider venom reveals new toxins with potential antimicrobial activity. *J. Proteomics* 151, 232–242. <https://doi.org/10.1016/j.jprot.2016.07.012>.
28. Luna-Ramirez, K., Tonk, M., Rahnamaeian, M., and Vilcinskis, A. (2017). Bioactivity of Natural and Engineered Antimicrobial Peptides from Venom of the Scorpions *Urodacus yaschenkoi* and *U. manicatus*. *Toxins* 9, 22. <https://doi.org/10.3390/toxins9010022>.
29. Lüddecke, T., Herzig, V., von Reumont, B.M., and Vilcinskis, A. (2022). The biology and evolution of spider venoms. *Biol. Rev.* 97, 163–178. <https://doi.org/10.1111/brv.12793>.
30. Herzig, V., King, G.F., and Undheim, E.A.B. (2019). Can we resolve the taxonomic bias in spider venom research? *Toxicon X* 1, 100005. <https://doi.org/10.1016/j.toxcx.2018.100005>.
31. Lüddecke, T., Vilcinskis, A., and Lemke, S. (2019). Phylogeny-Guided Selection of Priority Groups for Venom Bioprospecting: Harvesting Toxin Sequences in Tarantulas as a Case Study. *Toxins* 11, 488. <https://doi.org/10.3390/toxins11090488>.
32. von Reumont, B.M., Anderlüh, G., Antunes, A., Ayzvazyan, N., Beis, D., Caliskan, F., Crnković, A., Damm, M., Dutertre, S., Ellgaard, L., et al. (2022). Modern venomics-Current insights, novel methods, and future perspectives in biological and applied animal venom research. *GigaScience* 11, giac048. <https://doi.org/10.1093/gigascience/giac048>.
33. Rivera-de-Torre, E., Rimbault, C., Jenkins, T.P., Sørensen, C.V., Damsbo, A., Saez, N.J., Duho, Y., Hackney, C.M., Ellgaard, L., and Laustsen, A.H. (2021). Strategies for Heterologous Expression, Synthesis, and Purification of Animal Venom Toxins. *Front. Bioeng. Biotechnol.* 9, 811905. <https://doi.org/10.3389/fbioe.2021.811905>.
34. Lüddecke, T., Paas, A., Harris, R.J., Talmann, L., Kirchoff, K.N., Billion, A., Hards, K., Steinbrink, A., Gerlach, D., Fry, B.G., and Vilcinskis, A. (2023). Venom biotechnology: casting light on nature's deadliest weapons using synthetic biology. *Front. Bioeng. Biotechnol.* 11, 1166601. <https://doi.org/10.3389/fbioe.2023.1166601>.
35. Krämer, J., Lüddecke, T., Marner, M., Maiworm, E., Eichberg, J., Hards, K., Schäberle, T.F., Vilcinskis, A., and Predel, R. (2022). Antimicrobial, Insecticidal and Cytotoxic Activity of Linear Venom Peptides from the Pseudoscorpion *Chelifer cancrivorus*. *Toxins* 14, 58. <https://doi.org/10.3390/toxins14010058>.
36. Santibañez-López, C.E., Ontano, A.Z., Harvey, M.S., and Sharma, P.P. (2018). Transcriptomic Analysis of Pseudoscorpion Venom Reveals a Unique Cocktail Dominated by Enzymes and Protease Inhibitors. *Toxins* 10, 207. <https://doi.org/10.3390/toxins10050207>.
37. Stemme, T., and Pfeffer, S.E. (2021). Anatomy of the Nervous System in *Chelifer cancrivorus* (Arachnida: Pseudoscorpiones) with a Distinct Sensory Pathway Associated with the Pedipalps. *Insects* 13, 25. <https://doi.org/10.3390/insects13010025>.
38. Chamberlin (1924). Preliminary note upon the pseudoscorpions as a venomous order of the Arachnida. *Entomol. News* 35, 205–209.
39. Krämer, J., Pohl, H., and Predel, R. (2019). Venom collection and analysis in the pseudoscorpion *Chelifer cancrivorus* (Pseudoscorpiones: Cheliferidae). *Toxicon* 162, 15–23. <https://doi.org/10.1016/j.toxicon.2019.02.009>.
40. Krämer, J., Peigneur, S., Tytgat, J., Jenner, R.A., van Toor, R., and Predel, R. (2021). A Pseudoscorpion's Promising Pinch: The venom of *Chelifer cancrivorus* contains a rich source of novel compounds. *Toxicon* 201, 92–104. <https://doi.org/10.1016/j.toxicon.2021.08.012>.
41. Liu, G., Yang, F., Li, F., Li, Z., Lang, Y., Shen, B., Wu, Y., Li, W., Harrison, P.L., Strong, P.N., et al. (2018). Therapeutic Potential of a Scorpion Venom-Derived Antimicrobial Peptide and Its Homologs Against Antibiotic-Resistant Gram-Positive Bacteria. *Front. Microbiol.* 9, 1159. <https://doi.org/10.3389/fmicb.2018.01159>.
42. Pushpanathan, M., Gunasekaran, P., and Rajendran, J. (2013). Antimicrobial peptides: versatile biological properties. *Int. J. Pept.* 2013, 675391. <https://doi.org/10.1155/2013/675391>.
43. Wang, G., Li, X., and Wang, Z. (2016). APD3: the antimicrobial peptide database as a tool for research and education. *Nucleic Acids Res.* 44, D1087–D1093. <https://doi.org/10.1093/nar/gkv1278>.
44. Veltri, D., Kamath, U., and Shehu, A. (2018). Deep learning improves antimicrobial peptide recognition. *Bioinformatics* 34, 2740–2747.

- <https://doi.org/10.1093/bioinformatics/bty179>.
45. Jangir, P.K., Ogunlana, L., Szili, P., Czikkely, M., Shaw, L.P., Stevens, E.J., Yu, Y., Yang, Q., Wang, Y., Pál, C., et al. (2023). The evolution of colistin resistance increases bacterial resistance to host antimicrobial peptides and virulence. *Elife* 12, e84395.
 46. Ryan, R.Y.M., Seymour, J., Loukas, A., Lopez, J.A., Ikononopoulou, M.P., and Miles, J.J. (2021). Immunological Responses to Envenomation. *Front. Immunol.* 12, 661082. <https://doi.org/10.3389/fimmu.2021.661082>.
 47. Megaly, A.M.A., Yoshimoto, Y., Tsunoda, Y., Miyashita, M., Abdel-Wahab, M., Nakagawa, Y., and Miyagawa, H. (2021). Characterization of 2 linear peptides without disulfide bridges from the venom of the spider *Lycosa poonaensis* (Lycosidae). *Biosci. Biotechnol. Biochem.* 85, 1348–1356. <https://doi.org/10.1093/bbb/zbab046>.
 48. Dobson, A., Rowe, Z., Berger, J., Wholey, P., and Caro, T. (2021). Biodiversity loss due to more than climate change. *Science* 374, 699–700. <https://doi.org/10.1126/science.abm6216>.
 49. Hallmann, C.A., Sorg, M., Jongejans, E., Siepel, H., Hofland, N., Schwan, H., Stenmans, W., Müller, A., Sumser, H., Hören, T., et al. (2017). More than 75 percent decline over 27 years in total flying insect biomass in protected areas. *PLoS One* 12, e0185809. <https://doi.org/10.1371/journal.pone.0185809>.
 50. Nyffeler, M., and Bonte, D. (2020). Where Have All the Spiders Gone? Observations of a Dramatic Population Density Decline in the Once Very Abundant Garden Spider, *Araneus diadematus* (Araneae: Araneidae), in the Swiss Midland. *Insects* 11, 248. <https://doi.org/10.3390/insects11040248>.
 51. Gopal, R., Seo, C.H., Song, P.I., and Park, Y. (2013). Effect of repetitive lysine-tryptophan motifs on the bactericidal activity of antimicrobial peptides. *Amino Acids* 44, 645–660. <https://doi.org/10.1007/s00726-012-1388-6>.
 52. Hofer, A.M., and Lefkimiatis, K. (2007). Extracellular Calcium and cAMP: Second Messengers as “Third Messengers”? *Physiology* 22, 320–327. <https://doi.org/10.1152/physiol.00019.2007>.
 53. Gambardella, J., Khondkar, W., Morelli, M.B., Wang, X., Santulli, G., and Trimarco, V. (2020). Arginine and Endothelial Function. *Biomedicines* 8, 277. <https://doi.org/10.3390/biomedicines8080277>.
 54. Ghosh, A., Roy, R., Nandi, M., and Mukhopadhyay, A. (2019). Scorpion Venom-Toxins that Aid in Drug Development: A Review. *Int. J. Pept. Res. Ther.* 25, 27–37. <https://doi.org/10.1007/s10989-018-9721-x>.
 55. Shigenobu, S., and Wilson, A.C.C. (2011). Genomic revelations of a mutualism: the pea aphid and its obligate bacterial symbiont. *Cell. Mol. Life Sci.* 68, 1297–1309. <https://doi.org/10.1007/s00018-011-0645-2>.
 56. Luna-Ramirez, K., Skaljic, M., Grotmann, J., Kirfel, P., and Vilcinskas, A. (2017). Orally Delivered Scorpion Antimicrobial Peptides Exhibit Activity against Pea Aphid (*Acyrtosiphon pisum*) and Its Bacterial Symbionts. *Toxins* 9, 261. <https://doi.org/10.3390/toxins9090261>.
 57. Lüddecke, T., Schulz, S., Steinfartz, S., and Vences, M. (2018). A salamander’s toxic arsenal: review of skin poison diversity and function in true salamanders, genus *Salamandra*. *Naturwissenschaften* 105, 56. <https://doi.org/10.1007/s00114-018-1579-4>.
 58. Roelants, K., Fry, B.G., Ye, L., Stijlemans, B., Brys, L., Kok, P., Clynen, E., Schoofs, L., Cornelis, P., and Bossuyt, F. (2013). Origin and functional diversification of an amphibian defense peptide arsenal. *PLoS Genet.* 9, e1003662. <https://doi.org/10.1371/journal.pgen.1003662>.
 59. Daly, J.W. (1995). The chemistry of poisons in amphibian skin. *Proc. Natl. Acad. Sci. USA* 92, 9–13. <https://doi.org/10.1073/pnas.92.1.9>.
 60. Knepper, J., Lüddecke, T., Preißler, K., Vences, M., and Schulz, S. (2019). Isolation and Identification of Alkaloids from Poisons of Fire Salamanders (*Salamandra salamandra*). *J. Nat. Prod.* 82, 1319–1324. <https://doi.org/10.1021/acs.jnatprod.9b00065>.
 61. Ali, M.F., Soto, A., Knoop, F.C., and Conlon, J.M. (2001). Antimicrobial peptides isolated from skin secretions of the diploid frog, *Xenopus tropicalis* (Pipidae). *Biochim. Biophys. Acta* 1550, 81–89. [https://doi.org/10.1016/S0167-4838\(01\)00272-2](https://doi.org/10.1016/S0167-4838(01)00272-2).
 62. Yang, X., Lee, W.-H., and Zhang, Y. (2012). Extremely abundant antimicrobial peptides existed in the skins of nine kinds of Chinese odorless frogs. *J. Proteome Res.* 11, 306–319. <https://doi.org/10.1021/pr200782u>.
 63. Raaymakers, C., Verbrugghe, E., Hernot, S., Hellebuyck, T., Betti, C., Peleman, C., Claeys, M., Bert, W., Caveliers, V., Ballet, S., et al. (2017). Antimicrobial peptides in frog poisons constitute a molecular toxin delivery system against predators. *Nat. Commun.* 8, 1495. <https://doi.org/10.1038/s41467-017-01710-1>.
 64. Ul-Hasan, S., Rodríguez-Román, E., Reitzel, A.M., Adams, R.M.M., Herzig, V., Nobile, C.J., Saviola, A.J., Trim, S.A., Stiers, E.E., Moschos, S.A., et al. (2019). The emerging field of venom-microbiomics for exploring venom as a microenvironment, and the corresponding Initiative for Venom Associated Microbes and Parasites (iVAMP). *Toxicon* X 4, 100016. <https://doi.org/10.1016/j.toxcx.2019.100016>.
 65. Dunbar, J.P., Vitkauskaite, A., O’Keeffe, D.T., Fort, A., Sulpice, R., and Dugon, M.M. (2022). Bites by the noble false widow spider *Steatoda nobilis* can induce *Latrodectus*-like symptoms and vector-borne bacterial infections with implications for public health: a case series. *Clin. Toxicol.* 60, 59–70. <https://doi.org/10.1080/15563650.2021.1928165>.
 66. Gaver-Wainwright, M.M., Zack, R.S., Foradori, M.J., and Lavine, L.C. (2011). Misdiagnosis of spider bites: bacterial associates, mechanical pathogen transfer, and hemolytic potential of venom from the hobo spider, *Teegenaria agrestis* (Araneae: Agelenidae). *J. Med. Entomol.* 48, 382–388. <https://doi.org/10.1603/me09224>.
 67. Dunbar, J.P., Khan, N.A., Abberton, C.L., Brosnan, P., Murphy, J., Afoullous, S., O’Flaherty, V., Dugon, M.M., and Boyd, A. (2020). Synanthropic spiders, including the global invasive noble false widow *Steatoda nobilis*, are reservoirs for medically important and antibiotic resistant bacteria. *Sci. Rep.* 10, 20916. <https://doi.org/10.1038/s41598-020-77839-9>.
 68. Esmaeilshirazifard, E., Usher, L., Trim, C., Denise, H., Sangal, V., Tyson, G.H., Barlow, A., Redway, K.F., Taylor, J.D., Kremyda-Vlachou, M., et al. (2022). Bacterial Adaptation to Venom in Snakes and Arachnida. *Microbiol. Spectr.* 10, e02408-21. <https://doi.org/10.1128/spectrum.02408-21>.
 69. Pukala, T.L., Bertozzi, T., Donnellan, S.C., Bowie, J.H., Surinya-Johnson, K.H., Liu, Y., Jackway, R.J., Doyle, J.R., Llewellyn, L.E., and Tyler, M.J. (2006). Host-defence peptide profiles of the skin secretions of interspecific hybrid tree frogs and their parents, female *Litoria splendida* and male *Litoria caerulea*. *FEBS J.* 273, 3511–3519. <https://doi.org/10.1111/j.1742-4658.2006.05358.x>.
 70. Touchard, A., Aili, S.R., Fox, E.G.P., Escoubas, P., Orivel, J., Nicholson, G.M., and Dejean, A. (2016). The Biochemical Toxin Arsenal from Ant Venoms. *Toxins* 8, 30. <https://doi.org/10.3390/toxins8010030>.
 71. Gautier, R., Douquet, D., Antonny, B., and Drin, G. (2008). HELIQUEST: a web server to screen sequences with specific α -helical properties. *Bioinformatics* 24, 2101–2102. <https://doi.org/10.1093/bioinformatics/btn392>.
 72. Nguyen, L.-T., Schmidt, H.A., von Haeseler, A., and Minh, B.Q. (2015). IQ-TREE: a fast and effective stochastic algorithm for estimating maximum-likelihood phylogenies. *Mol. Biol. Evol.* 32, 268–274. <https://doi.org/10.1093/molbev/msu300>.
 73. Balouiri, M., Sadiki, M., and Ibsouda, S.K. (2016). Methods for *in vitro* evaluating antimicrobial activity: A review. *J. Pharm. Anal.* 6, 71–79. <https://doi.org/10.1016/j.jppha.2015.11.005>.

STAR★METHODS

KEY RESOURCES TABLE

REAGENT or RESOURCE	SOURCE	IDENTIFIER
Bacterial and virus strains		
<i>Escherichia coli</i>	ATCC (Manassas, VA, USA)	ATCC35218
<i>Pseudomonas aeruginosa</i>	ATCC (Manassas, VA, USA)	ATCC27853
<i>Mycobacterium smegmatis</i>	ATCC (Manassas, VA, USA)	ATCC607
<i>Staphylococcus aureus</i>	ATCC (Manassas, VA, USA)	ATCC33592
<i>Aspergillus flavus</i>	ATCC (Manassas, VA, USA)	ATCC9170
<i>Candida albicans</i>	Fraunhofer IME Strain Collection (Gießen, Germany)	FH2173
Chemicals, peptides, and recombinant proteins		
Synthetic Checacins	GenScript Biotech (Piscataway, NJ, USA)	Checacin1 - 6, NCVC11
Critical commercial assays		
Orangu assay	Cell Guidance Systems, Cambridge, UK	
BacTiter-Glo assay	Promega, Madison, WI, USA	
Experimental models: Cell lines		
HEK293T	Leibniz Institute German Collection of Microorganisms and Cell Cultures (DSMZ, Braunschweig, Germany)	
MDA-MB-231	Leibniz Institute German Collection of Microorganisms and Cell Cultures (DSMZ, Braunschweig, Germany)	
RAW246.7	ATCC (Manassas, VA, USA)	
NHDF	PELOBiotech (Martinsried, Germany)	
HeLa	Prof. Dr. Rolf Marschalek	W1/21Fü
Recombinant DNA		
pGloSensor-22F cAMP	Promega, Madison, WI, USA	
Software and algorithms		
Geneious v10.2.6	Dotmatics	
HeliQuest	Institut de pharmacologie moléculaire et cellulaire	
Antimicrobial Peptide Database 3	University of Nebraska Medical Center	
AMP scanner vr.2	https://www.dveltri.com/ascan/v2/ascan.html	
IQ-TREE	Center for Integrative Bioinformatics Vienna	
GraphPad Prism v8	GraphPad Software, San Diego, CA, USA	

RESOURCE AVAILABILITY

Lead contact

Further information and requests for resources and information should be directed to and will be fulfilled by Tim Lüddecke (tim.lueddecke@ime.fraunhofer.de).

Materials availability

Peptides generated in this study are available on request contacting Tim Lüddecke (tim.lueddecke@ime.fraunhofer.de).

Data and code availability

- Raw data derived from *in vitro* experiments are available as supplementary files adjacent to this article.
- This paper does not report original code.

METHOD DETAILS

Checacins

The sequences of eight checacins were retrieved from a previous study.³⁹ For *in vitro* experiments, peptides were synthesized by GenScript Biotech (Piscataway, NJ, USA) including HPLC-based analysis of purity and mass spectrometry to verify identity (Table S3).

In silico analysis

Secondary structures were predicted using the Garnier tool of EMBOSS v6.5.7 in Geneious v10.2.6. A deeper analysis of helical potential was carried out using HeliQuest with the full sequence as the window size.⁷¹ To predict antimicrobial activity, all sequences were analyzed using the AMP calculator and predictor tool in AMP database 3⁴³ and AMP scanner vr.2.⁴⁴ Raw data created by all software is given in Table S1.

Molecular phylogeny

Full precursor nucleotide sequences of checacins and megicin 18 were aligned using Clustal W in Geneious v10.2.6 and were uploaded to the IQ-TREE webserver.⁷² A maximum likelihood tree was calculated using DNA as the sequence type and the best-fitting substitution model selected in Auto mode. Branch analysis was achieved by ultrafast bootstrap support using 10,000 replicates and an activated SH-aLRT branch test. We selected a perturbation strength of 0.5, and the IQ-TREE stopping rule was set to 100. From the resulting tree space, a 65% majority rule consensus tree was created and visualized using Figtree v1.4.4. The resulting tree was rooted using the related scorpion toxin megicin 18 as an outgroup.

Antimicrobial activity

Antimicrobial activities were determined using a method recommended by the EUCAST committee.⁷³ The MIC was defined as the lowest concentration inhibiting microbial growth by 85% after subtracting background signals from the medium. We dissolved the peptides in sterile ultra-pure water (0.055 $\mu\text{S}/\text{cm}$) and examined their effects in a dilution series from 50 to 0.02 μM . We used rifampicin, tetracycline and gentamicin (Sigma-Aldrich, St. Louis, MO, USA) as positive controls and applied them in a dilution series from 64 to 0.03 $\mu\text{g}/\text{mL}$. Untreated bacteria were used as negative controls. All measurements were carried out in triplicates. *E. coli* (ATCC35218), *S. aureus* (ATCC33592) and *P. aeruginosa* (ATCC27853) were incubated overnight at 37°C and 85% relative humidity, shaking at 180 rpm, before dilution to 5×10^5 cells/mL in cation-adjusted Mueller Hinton II (MHII) medium (Becton Dickinson, Sparks, NV, USA). A second *E. coli* suspension was prepared in cation-adjusted MHII medium mixed with 44 mM sodium bicarbonate (MHC). After incubation as above, we measured the turbidity at 600 nm on a LUMIstar Omega microplate spectrophotometer (BMG Labtech, Ortenberg, Germany). The *M. smegmatis* (ATCC607) pre-culture was incubated in brain–heart infusion (BHI) broth (Becton Dickinson) for 48 h as above before the cell concentration was adjusted in MHII medium. Isoniazid (Sigma-Aldrich) was used instead of gentamicin as the third positive control. *C. albicans* (FH2173) was incubated for 48 h at 28°C, shaking at 180 rpm, before the pre-culture was diluted to 1×10^5 cells/mL in MHII medium. For *A. flavus* (ATCC9170), a previously prepared spore solution was used to adjust the assay inoculum to 1×10^5 spores/mL. Assays were incubated for 48 h at 37°C, shaking at 180 rpm. Tebuconazole (Cayman Chemical Company, Ann Arbor, MI, USA), amphotericin B, and nystatin (both Sigma-Aldrich) were used as positive controls (dilution series 64 to 0.03 $\mu\text{g}/\text{mL}$) for both fungi. In all cases (*M. smegmatis*, *C. albicans*, *A. flavus*), cell viability was evaluated after 48 h by measuring ATP levels using the BacTiter-Glo assay (Promega, Madison, WI, USA) according to the manufacturer's instructions.

Cells and reagents

HEK293T and MDA-MB-231 (ACC-732) cells were purchased from the Leibniz Institute German Collection of Microorganisms and Cell Cultures (DSMZ, Braunschweig, Germany). RAW246.7 cells and NHDFs were purchased from the ATCC (Manassas, VA, USA) and PELOBiotech (Martinsried, Germany), respectively. The HeLa cells were a generous gift from Prof. Dr. Rolf Marschalek. Primary HUVECs were isolated from human umbilical cords. The head of the Research Ethics Committee/Institutional Review Board (REC/IRB) granted a waiver for the use of anonymized human material on September 15, 2021, under reference number W1/21Fü. HEK293T, MDA-MB-231, HeLa and NHDF cells were cultivated in Dulbecco's modified Eagle's medium (DMEM) and RAW246.7 cells in Roswell Park Memorial Institute (RPMI) medium. All media were supplemented with 10% fetal calf serum (FCS; Biochrom, Berlin, Germany), and 1% penicillin/streptomycin. Primary HUVECs were cultured in 75 cm² flasks coated with collagen G (Biochrom) in endothelial cell growth medium (PELOBiotech) supplemented with 10% FCS (Biochrom), 100 U/mL penicillin, 100 $\mu\text{g}/\text{mL}$ streptomycin, and 2.5 $\mu\text{g}/\text{mL}$ amphotericin B (PAN-Biotech, Aidenbach, Germany), and a supplement mixture (PELOBiotech). All cells were cultured at 37°C in a 5% CO₂ atmosphere.

Cell viability assay

Cell viability was measured using the Orangu assay (Cell Guidance Systems, Cambridge, UK). Briefly, 2×10^5 HEK293T or RAW246.7 cells seeded in 96-well plates were treated with various concentrations of the checacins or water as a control for 24 h before adding 10 μl Orangu cell counting solution and incubating for 60 min. The absorbance was measured at 450 nm with a reference at 650 nm using an EnSpire 2300 Multimode Plate Reader (Perkin Elmer, Lübeck, Germany). Cell viability was calculated as a percentage compared to the water-treated cells (100%). Raw data of cell viability assays is given in Table S2.

Cell proliferation assay

HUVECs, NHDFs, MDA-MB-231 and HeLa cells were treated with checacins or water as a control. HUVECs (2000 cells/well) were seeded into collagen-coated 96-well plates and grown for 24 h before treatment. Treated cells were cultured for 72 h before fixation in 2:1 methanol/ethanol, washing in PBS, and staining with 20% crystal violet in methanol. Control cells were similarly processed after 24 h. Unbound crystal violet was removed by washing with distilled water. Finally, cells were left to air dry, and DNA-bound crystal violet was dissolved in 20% acetic acid and quantified by measuring the absorbance at 590 nm using an Infinite F200Pro plate reader (Tecan, Männedorf, Switzerland). The inhibition of proliferation was calculated as a percentage relative to the water control (100%) and was also compared to DMSO controls (0.01% or 0.025%) after 72 h incubation. Similarly, MDA-MB-231 cells (5×10^3 cells/well), HeLa cells (2.5×10^3 cells/well) and NHDFs (1.5×10^3 cells/well) were seeded into 96-well plates, and proliferation was tested as described above. Raw data of cell proliferation assays is given in [Table S2](#).

Analysis of intracellular Ca^{2+} levels

Ca^{2+} release was analyzed by labeling cells with the calcium fluorescence probe Fluo-8-AM. Briefly, 2×10^4 HEK293T cells were seeded into 96-well poly-D-lysine plates and cultured at 37°C for 24 h before adding $4 \mu\text{M}$ Fluo-8-AM in Hanks' balanced salt solution (HBSS) for 1 h at 37°C . The Fluo-8/HBSS medium was then replaced with $100 \mu\text{l}$ HBSS. Five images per second were captured using an ImageXpress Micro confocal high-content imaging system (Molecular Devices, San Jose, CA, USA). For the induction assay, the cells were treated with checacins or $5 \mu\text{M}$ ionomycin (Sigma-Aldrich) as a positive control, and images were captured every second for 20 s. For the inhibition assay, $5 \mu\text{M}$ ionomycin was added to the checacin samples after 30 min and images were captured as above. Data were analyzed using MetaXpress software. The fluorescence intensity threshold was defined using cells before treatment, and all cells with a signal above the threshold level were counted. For the induction assay, the number of cells above the threshold in the checacin-treated samples was compared to the untreated sample. For the inhibition assay, the number of cells above the threshold in the checacin-treated samples was compared to the cells in the ionomycin-treated sample. Raw data of Ca^{2+} release assays is given in [Table S2](#).

Analysis of cAMP levels

HEK293T cells were transfected with the pGloSensor-22F cAMP vector (Promega) using turbofect reagent (Thermo Fisher Scientific, Frankfurt am Main, Germany). We then seeded plates with 7×10^4 transfected cells and incubated for 24 h before replacing the supernatant with DMEM lacking phenol red and supplemented with the pGlo sensor cAMP reagent (Promega). Induction and inhibition assays were carried out in two steps on the same plate. For the induction assay, luminescence was detected (background, three measurements every 5 min) before adding checacin peptides or $5 \mu\text{M}$ forskolin and repeating the measurements using a Spark plate reader (Tecan). For the inhibition assay, cells pre-treated with each checacin peptide were incubated with $5 \mu\text{M}$ forskolin and luminescence was detected as above. The luminescence values of the checacin-treated samples were compared to samples treated with DMSO or forskolin. Raw data of cAMP assays is given in [Table S2](#).

Analysis of NO levels

NO was quantified using the Griess method as previously described.⁸ Briefly, 2×10^4 RAW264.7 macrophages per well were seeded in a 96-well plate and incubated for 24 h at 37°C . Checacins at various concentrations or 100 ng/ml lipopolysaccharide (LPS) as a positive control were added to induce NO synthesis. Alternatively, cells pre-treated with checacins for 30 min were incubated with 100 ng/ml LPS to investigate the inhibition of NO synthesis. After 24 h, supernatants were collected and stored at -80°C . A standard curve was prepared using different concentrations of sodium nitrite ($0\text{--}50 \mu\text{M}$). We then added $80 \mu\text{l}$ cell supernatant or standard to a 96-well microplate and incubated with $20 \mu\text{l}$ sulfanilamide solution (40 mg/ml in 1 M HCl) and $20 \mu\text{l}$ naphthylethylenediamine solution (60 mg/ml *N*-(1-naphthyl)ethylenediamine dihydrochloride in water) for 15 min. The absorbance was measured at 540 nm using an EnSpire Plate Reader. Raw data of NO release assays is given in [Table S2](#).

QUANTIFICATION AND STATISTICAL ANALYSIS

Data were processed and visualized using GraphPad Prism v8 (GraphPad Software, San Diego, CA, USA). Results are presented as means \pm standard errors of the mean (SEM). The number of independently performed experiments (n) is stated in the figure captions, and at least three technical replicates were used for the experiments. Statistical significance was determined by one-way or two-way analysis of variance (ANOVA) with Dunnett's multiple comparisons test and Tukey's *post hoc* test. The threshold for significance was $p < 0.05$.